The EMBO Journal (2010) 29, 2276–2289 | © 2010 European Molecular Biology Organization | Some Rights Reserved 0261-4189/10
www.embojournal.org

THE EMBO JOURNAL

EMBO open

Regulation of dynamic polarity switching in bacteria by a Ras-like G-protein and its cognate GAP

Simone Leonardy[1], Mandy Miertzschke[2], Iryna Bulyha[1], Eva Sperling[1], Alfred Wittinghofer[2] and Lotte Søgaard-Andersen[1,*]

[1]Department of Ecophysiology, Max Planck Institute for Terrestrial Microbiology, Marburg, Germany and [2]Department of Structural Biology, Max Planck Institute for Molecular Physiology, Dortmund, Germany

The rod-shaped cells of the bacterium *Myxococcus xanthus* move uni-directionally and occasionally undergo reversals during which the leading/lagging polarity axis is inverted. Cellular reversals depend on pole-to-pole relocation of motility proteins that localize to the cell poles between reversals. We show that MglA is a Ras-like G-protein and acts as a nucleotide-dependent molecular switch to regulate motility and that MglB represents a novel GTPase-activating protein (GAP) family and is the cognate GAP of MglA. Between reversals, MglA/GTP is restricted to the leading and MglB to the lagging pole defining the leading/lagging polarity axis. For reversals, the Frz chemosensory system induces the relocation of MglA/GTP to the lagging pole causing an inversion of the leading/lagging polarity axis. MglA/GTP stimulates motility by establishing correct polarity of motility proteins between reversals and reversals by inducing their pole-to-pole relocation. Thus, the function of Ras-like G-proteins and their GAPs in regulating cell polarity is found not only in eukaryotes, but also conserved in bacteria.

The EMBO Journal (2010) **29,** 2276–2289. doi:10.1038/emboj.2010.114; Published online 11 June 2010
Subject Categories: signal transduction; microbiology & pathogens
Keywords: cell polarity; dynamic protein localization; GTPase-activating protein; Ras-like GTPase; type IV pili

Introduction

Cell polarity is a fundamental property of all cells and involves establishing and maintaining the spatial asymmetry of macromolecules (Rafelski and Marshall, 2008). An important consequence of cell polarity is that the activity of asymmetrically localized proteins is spatially confined, thus, laying the foundation for processes that require the localized activity of a protein or protein complexes (Nelson, 2003; Gitai *et al*, 2005). Cell polarity touches on essentially every aspect of cell function and the processes in which polarity has a decisive function are remarkably similar in eukaryotic cells and bacteria and include cell growth, cell cycle control, division, differentiation, and motility (Etienne-Manneville and Hall, 2002; Gitai *et al*, 2005; Shapiro *et al*, 2009).

Major questions in understanding cell polarity are how proteins find their correct localization and how this localization may change dynamically over time. In eukaryotic cells, Ras-like G-proteins, which can be divided into five major subfamilies (Ras, Rho, Rab, Arf, and Ran) (Leipe *et al*, 2002), have essential functions in establishing and maintaining cell polarity. These proteins are binary molecular switches that cycle between an inactive GDP- and an active GTP-bound state (Bourne *et al*, 1991). The nucleotide-bound state is regulated by guanine nucleotide exchange factors (GEFs) that catalyse the intrinsically slow exchange of GDP for GTP, and GTPase-activating proteins (GAPs), which stimulate the low intrinsic GTPase activity (Bourne *et al*, 1991). GTP binding induces a conformational change in Ras-like proteins, thereby promoting their interaction with effectors that control or are part of downstream pathways to elicit a particular response (Wittinghofer and Nassar, 1996). Often the activity of Ras-like G-proteins is temporally and spatially regulated. For example, in *Dictyostelium discoideum* Ras activation occurs at the leading edge of cells exposed to a gradient of chemoattractant (Charest and Firtel, 2007) and in *Saccharomyces cerevisiae*, Cdc42, a master regulator of cell polarity conserved from yeast to mammals, is activated at the incipient bud site (Etienne-Manneville, 2004).

Over the last 10 years, it has become clear that bacteria are spatially highly organized and, thus, display cell polarity (Gitai *et al*, 2005; Shapiro *et al*, 2009). Spatially organized elements of bacteria include proteins as well as the chromosome (Viollier *et al*, 2004). Little is known about how polarity in bacteria is established and maintained. However, some principles are emerging for polarized proteins. First, protein localization may be positively regulated by *trans*-acting targeting factors (Shapiro *et al*, 2009) as shown for DivIVA, which directly recruits MinJ to the cell poles in *Bacillus subtilis* (Bramkamp *et al*, 2008; Patrick and Kearns, 2008). Second, localization may be negatively regulated as in the case of the cell division machinery. In this process, negative regulators inhibit FtsZ-ring formation in the entire cell with

*Corresponding author. Department of Ecophysiology, Max Planck Institute for Terrestrial Microbiology, Karl-von-Frisch Strasse 10, Marburg 35043, Germany. Tel. +49 6421 178201; Fax +49 6421 178209; E-mail: sogaard@mpi-marburg.mpg.de

Received: 4 April 2010; accepted: 10 May 2010; published online: 11 June 2010

the exception of the incipient division site (Lutkenhaus, 2007). Third, some localized proteins interact with proteins that bind to specific sites on the chromosome (Thanbichler and Shapiro, 2008). As the chromosome is spatially organized, this interaction results in localization of the interacting protein. Finally, a mechanism for protein localization involving recognition of membranes of positive or negative curvature was proposed for some peripheral membrane proteins in *B. subtilis* (Shapiro *et al*, 2009). Except for proteins involved in cell cycle regulation and cell division, most polarized proteins in bacteria are not dynamically localized and do not change localization over time (Shapiro *et al*, 2009). The dynamic localization of these proteins depends on specific cell cycle events, which by largely unknown mechanisms trigger protein relocalization (Shapiro *et al*, 2009). Many dynamically localized proteins are restricted to the cell poles or the division site, and it has been proposed that proteins targeted to a cell pole by the earlier cell division could act as targeting factors for other polarly localized proteins as in the case of the TipN protein in *Caulobacter crescentus* (Huitema *et al*, 2006; Lam *et al*, 2006). Cells of the rod-shaped bacterium *Myxococcus xanthus* provide a simple experimental system to address how bacterial cell polarity and dynamic protein localization is accomplished because these cells switch their leading/lagging pole polarity axis frequently and independently of the cell cycle to regulate cell motility.

M. xanthus cells organize into two patterns, spreading colonies in the presence of nutrients and fruiting bodies in the absence of nutrients. Formation of both patterns depends on regulation of motility (Leonardy *et al*, 2008). *M. xanthus* has two motility systems, type IV pili (T4P) (Wu and Kaiser, 1995) and the A-engine (Hodgkin and Kaiser, 1979), which act synergistically (Kaiser and Crosby, 1983). *M. xanthus* cells move uni-directionally on surfaces; occasionally, however, cells stop and then resume motility in the opposite direction, with the old leading cell pole becoming the new lagging pole (Blackhart and Zusman, 1985). These events are referred to as reversals and at the cellular level a reversal corresponds to an inversion of the leading/lagging pole polarity axis. Cellular reversals are stochastic events, not coupled to the cell cycle, and the reversal frequency is regulated by the Frz chemosensory system (Blackhart and Zusman, 1985). Moreover, proper regulation of the reversal frequency is essential for formation of both cellular patterns (Blackhart and Zusman, 1985).

In *M. xanthus*, T4P are assembled at the leading pole, and during a reversal, this pole changes (Sun *et al*, 2000; Mignot *et al*, 2005; Bulyha *et al*, 2009). Between reversals, the ATPase PilT that energizes T4P retractions localize at the lagging pole, whereas the ATPase PilB, which catalyses T4P extension, and the FrzS protein, which has an unknown function in T4P function, localize at the leading pole. During reversals, these three proteins relocate between the poles. Several other T4P proteins localize in bipolar, symmetric clusters, which remain stationary at the poles during reversals (Bulyha *et al*, 2009).

It is not known how force is generated in the A-motility system. However, this motility system also depends on polar localization of proteins between reversals and their dynamic relocalization between poles during reversals as shown for the two A-motility proteins, AglZ and RomR, which have unknown functions in A-motility. Between reversals, AglZ localizes in a large cluster at the leading pole and smaller clusters, also referred to as focal adhesion complexes, along the cell body (Mignot *et al*, 2007) and RomR localizes with a large cluster at the lagging pole (Leonardy *et al*, 2007). During reversals, these polar clusters relocate in opposite direction between the poles. Thus, at the molecular level, a cellular reversal corresponds to the inversion of the polarity axis of proteins of T4P as well as of the A-engine.

The MglA protein is important for the function of both motility systems (Hodgkin and Kaiser, 1979). MglA shares homology to Ras-like G-proteins (Hartzell and Kaiser, 1991; Leipe *et al*, 2002) and is a member of the sixth major subfamily of these proteins (Leipe *et al*, 2002). Recently, it was found that MglA influences the polarity of motility proteins and in an *mglA* mutant RomR localizes in a single cluster at the 'wrong pole', that is the pole containing T4P (Leonardy *et al*, 2007) and AglZ in a mostly diffuse pattern (Mauriello *et al*, 2010). It has also been shown that MglA has GTPase activity (Mauriello *et al*, 2010). These observations taken together with the knowledge that Ras-like proteins function in cell polarity in eukaryotes made us hypothesize that MglA is involved in regulating the polarity of motility proteins. Here, we show that MglA is a nucleotide-dependent molecular switch and that MglB, which is encoded in an operon with MglA, is a MglA-specific GAP. MglA/GTP represents the active form and stimulates motility by setting up the correct polarity of motility proteins. Further accumulation of MglA/GTP induces reversals by stimulating pole-to-pole relocation of motility proteins. MglA activity is controlled temporally and spatially by the Frz system and the MglAGAP MglB.

Results

MglA is a nucleotide-dependent molecular switch

The molecular mass of MglA (22 kDa) is Ras like, and MglA contains most of the conserved canonical residues required for guanine nucleotide binding and GTP hydrolysis observed in Ras-like G-proteins. The major differences are the absence of a Thr residue in the switch I region and the absence of the highly conserved Asp in the DxxGQ motif in the switch II region (Supplementary Figure S1).

The analysis of mutants stabilized in the GTP-bound form as well as dominant-negative and inactive mutants have provided insights into the *in vivo* function of Ras-like proteins in eukaryotic cells. We used a similar approach to analyse the importance of the GTPase cycle of MglA and generated MglA mutants with presumably similar effects on nucleotide binding and/or hydrolysis. The $MglA^{G21V}$ mutant has a substitution in the P-loop corresponding to the oncogenic Ras^{G12V} mutant and is predicted to be permanently in the GTP-bound active state because both the intrinsic and even more significantly the GAP-stimulated GTPase activity is dramatically reduced (Scheffzek *et al*, 1997; Vetter and Wittinghofer, 2001). The $MglA^{T26/27N}$ mutant was designed based on the assumption that its properties are similar to the Ras^{S17N} mutant, which has a lower affinity for GTP than for GDP, and is in general much less stable because of the absence of the residue coordinating the Mg^{2+} ion. However, it is not necessarily locked in the GDP-bound state and its major defects seem to be the reduced binding of nucleotides and tight binding to GEF (John *et al*, 1993; Cool *et al*, 1999; Feig,

1999). In MglA, T26 corresponds to S17 in Ras. To exclude that T27 in MglA would take over the function of T26 and coordinate the Mg^{2+} ion, T26 as well as T27 were substituted to N in $MglA^{T26/27N}$.

To confirm that MglA functions as a Ras-like G-protein and to characterize the mutant proteins, we attempted to purify the wild type (wt) and mutant *M. xanthus* proteins after overexpression in *Escherichia coli*. However, in our hands, all three proteins were mostly insoluble. Even the soluble fraction could not be purified to homogeneity and tended to aggregate at higher concentrations. *Thermus thermophilus* contains an *mglBA* operon encoding MglA and MglB proteins that are 62/81% and 28/52% identical/similar to MglA and MglB of *M. xanthus*, respectively (Supplementary Figure S1). The *T. thermophilus* MglA and MglB proteins (see below) were expressed and purified in soluble form and did not aggregate (Figure 1A). We, therefore, investigated the biochemical properties of the MglA/B proteins using the homologues from *T. thermophilus*.

Nucleotide binding is conveniently measured using *N*-methylanthraniloyl (m, mant)-labelled nucleotides. Although not all the canonical residues of eukaryotic Ras-like G-proteins are conserved, nucleotide-free $MglA^{+}$ nevertheless bound mGDP and mGTP as well as the non-hydrolysable GTP analogue mGppNHp with nanomolar affinities, whereas mADP and mATP were bound with much lower affinities, which could not be quantified with confidence (Figure 1B). $MglA^{G21V}$ and $MglA^{T26/27N}$ were not significantly affected in nucleotide binding except that $MglA^{T26/27N}$ bound mGTP and mGppNHp with strongly reduced affinity (Figure 1B). To determine whether MglA has GTPase activity, the release of P_i from [γ-^{32}P]GTP was measured. As is characteristic for Ras-like G-proteins, $MglA^{+}$ showed a slow intrinsic GTPase reaction with a half-life of about 80 min, which is reduced about seven-fold in the case of $MglA^{G21V}$ (Figure 1C). This supports the hypothesis that $MglA^{+}$ is a G-protein with properties similar to Ras-like proteins and that $MglA^{G21V}$ corresponds to the oncogenic-activating Ras^{G12V} mutant. The $MglA^{T26/27N}$ mutant showed an even more reduced intrinsic GTPase reaction (Figure 1C). In conjunction with the strongly reduced mGTP and mGppNHp affinities, we predict that *M. xanthus* $MglA^{T26/27N}$ is a loss of function and dominant-negative mutant of MglA because of loss of stability, tight interaction with a respective GEF, and/or disturbed interaction with downstream effectors similar to the corresponding mutants of Ras-like proteins (John *et al*, 1993; Cool *et al*, 1999; Feig, 1999).

mglA is in an operon with the upstream *mglB* gene (Stephens *et al*, 1989), and it has been reported that MglB is important for accumulation of MglA (Hartzell and Kaiser, 1991). Therefore, the $mglA^{G21V}$ and $mglA^{T26/27N}$ alleles were expressed together with *mglB* after integration at the *M. xanthus* phage Mx8 attachment site in both wt and in a Δ*mglBA* mutant. Using time-lapse microscopy, we found that wt cells moved with an average velocity of $3.2 \pm 0.3\ \mu m\ min^{-1}$ and reversed their direction with an average reversal period of 13.9 min (Table Ia). The Δ*mglBA* mutant was non-motile. Expression of $mglBA^{+}$ and $mglBA^{G21V}$ at native levels (Supplementary Figure S2) corrected the motility defects caused by Δ*mglBA*; however, $mglA^{G21V}$ cells reversed approximately three-fold more frequently than wt and with an average reversal period of 4.6 min. However, $mglBA^{T26/27N}$ did not complement the motility defects caused by Δ*mglBA*. Similar results were obtained when $MglA^{G21V}$ and $MglA^{T26/27N}$ were synthesized from the native chromosomal site. Merodiploid $mglA^{+}$, $mglA^{G21V}$ cells moved at wt velocities, but hyper-reversed similarly to the mutant only accumulating $MglA^{G21V}$ (Table Ia). Merodiploid $mglA^{+}$, $mglA^{T26/27N}$ cells also moved at wt velocities, but only reversed every 48 min. Thus, the mutant *mglA* alleles are dominant over $mglA^{+}$ with respect to reversals. Taken together with the biochemical characteristics of the three MglA proteins, these data are in agreement with the hypothesis that MglA functions as a nucleotide-dependent molecular switch

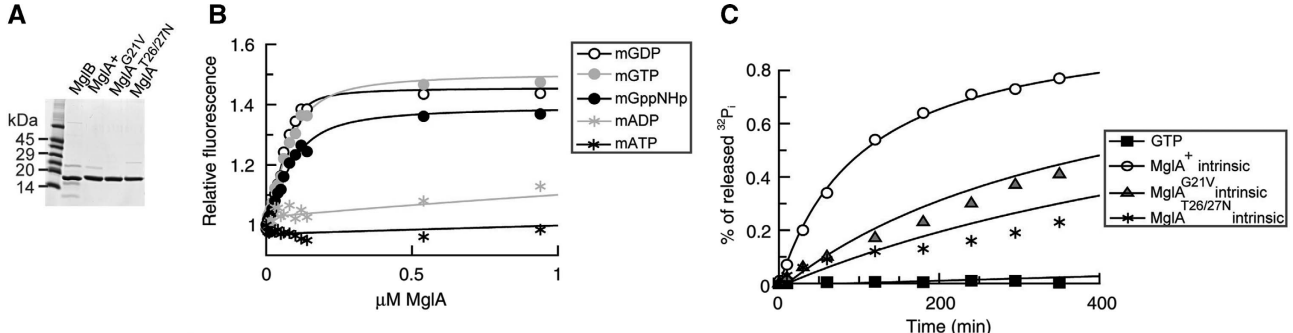

K_d in μM	$MglA^{+}$	$MglA^{G21V}$	$MglA^{T26/27N}$
mGDP	0.0073 ± 0.0013	0.0047 ± 0.0014	0.0075 ± 0.0034
mGTP	0.0246 ± 0.0030	0.0191 ± 0.0026	1.6588 ± 0.3195
mGppNHp	0.0328 ± 0.0045	0.0074 ± 0.0042	3.7424 ± 0.8857

Figure 1 MglA is a Ras-like G-protein. (**A**) Purification of MglB, $MglA^{+}$, $MglA^{G21V}$, and $MglA^{T26/27N}$ of *T. thermophilus*. Total purified protein separated by SDS–PAGE (5 μg protein loaded per lane). Migration of molecular size markers is indicated on the left. MglB and MglA have calculated molecular masses of 17 and 22 kDa, respectively. (**B**) MglA binds with high affinity to mant-labelled G-nucleotides. A total of 0.1 μM mGDP, mGTP, mGppNHp, mADP and mATP were titrated with nucleotide-free MglA and binding affinities determined by measuring the relative fluorescence intensities. The K_d's for binding to mGDP, mGTP, and mGppNHp of $MglA^{+}$, $MglA^{G21V}$, and $MglA^{T26/27N}$ are indicated below. (**C**) MglA has slow intrinsic GTPase activity. Graph depicts the release of $^{32}P_i$ using the charcoal assay with [γ-^{32}P]GTP and 4 μM of $MglA^{+}$, $MglA^{G21V}$, and $MglA^{T26/27N}$ over time (min).

Table I Motility characteristics of *mglA*, *mglB*, and *frz* mutants

Strain	Genotype[a]	Reversal period (min)	Velocity ($\mu m\ min^{-1}$)
(a)			
DK1622	*mglBA*$^+$	13.9	3.2 ± 0.3
DK6204	Δ*mglBA*	NA	NA
SA3302	Δ*mglBA*/*mglBA*$^+$	14.2	3.5 ± 0.5
SA3303	Δ*mglBA*/*mglBA*^{G21V}	4.6	2.6 ± 0.2
SA3304	Δ*mglBA*/*mglBA*$^{T26/27N}$	NA	NA
SA3306	*mglBA*$^+$/*mglBA*$^+$	14.0	3.6 ± 0.2
SA3307	*mglBA*$^+$/*mglBA*^{G21V}	4.7	3.0 ± 0.3
SA3308	*mglBA*$^+$/*mglBA*$^{T26/27N}$	48	3.4 ± 0.7
SA3334	*mglBA*^{G21V}	4.6	3.1 ± 0.5
SA3335	*mglBA*$^{T26/27N}$	NA	NA
(b)			
DK8505	*frz*^{lof}, *mglBA*$^+$	>100	2.2 ± 0.4
SA3325	*frz*^{lof}, Δ*mglBA*	NA	NA
SA3318	*frz*^{lof}, Δ*mglBA*/*mglBA*^{G21V}	5.7	2.3 ± 0.3
SA3321	*frz*^{lof}, Δ*mglBA*/*mglBA*$^{T26/27N}$	NA	NA
DK8506	*frz*^{gof}, *mglBA*$^+$	1.5	2.4 ± 0.5
SA3324	*frz*^{gof}, Δ*mglBA*	NA	NA
SA3319	*frz*^{gof}, Δ*mglBA*/*mglBA*^{G21V}	5.0	1.6 ± 0.2
SA3320	*frz*^{gof}, Δ*mglBA*/*mglBA*$^{T26/27N}$	NA	NA
(c)			
DK3685	*mglA9*	NA	NA
SA2096	*mglA9*/*mglA*$^+$	13.8	3.0 ± 0.4
SA3359	*mglA9*/*yfp–mglA*$^+$	12.9	2.8 ± 0.2
SA3360	*mglA9*/*yfp–mglA*^{G21V}	4.7	2.4 ± 0.3
SA3361	*mglA9*/*yfp–mglA*$^{T26/27N}$	NA	NA
(d)			
SA3387	Δ*mglB*	6.5	3.0 ± 0.4
SA3388	Δ*mglB*/*mglB–yfp*	12.4	2.8 ± 0.2
SA3385	Δ*mglBA*/*yfp–mglA*$^+$	6.8	2.4 ± 0.3
SA3386	Δ*mglBA*/*mglB–yfp*	NA	NA

NA, not applicable.
[a]*frz*^{lof} and *frz*^{gof} alleles are *frzCD*::Tn*5lac*Ω536 and *frzCD*::Tn*5*Ω224, respectively.

in which MglA/GTP represents the active form stimulating motility as well as reversals and MglA$^{T26/27N}$, an inactive and dominant-negative form.

MglA acts downstream of the Frz chemosensory system to induce cellular reversals

Frz regulates the reversal frequency, but is not required for motility *per se*. To determine whether Frz and MglA act in the same or in parallel pathways to induce reversals, we performed genetic epistasis tests (Table Ib). As earlier reported, cells containing *frz*^{lof} (loss-of-function) or *frz*^{gof} (gain-of-function) alleles rarely reversed and hyper-reversed, respectively. Importantly, the *frz*^{lof}, *mglA*^{G21V} mutant had a hyper-reversing phenotype similar to that of the *frz*$^+$, *mglA*^{G21V} mutant. In addition, the *frz*^{gof}, *mglA*^{G21V} mutant reversed with the same reversal period as *frz*$^+$, *mglA*^{G21V} cells. Moreover, all strains containing the *mglA*$^{T26/27N}$ allele were non-motile. Thus, *mglA*^{G21V} bypasses *frz*^{lof} for reversals and the *frz*^{gof} and *mglA*^{G21V} mutations do not cause an additive phenotype. These observations suggest that Frz and MglA act in the same pathway and that MglA acts downstream of Frz to induce reversals. These data also show that MglA/GTP has two separable activities. One activity is stimulation of motility and this activity is independent of Frz. The second activity is stimulation of reversals and this activity depends on Frz.

MglA localizes to the leading pole and relocates before reversals

As MglA stimulates motility and reversals, we speculated that MglA activity is spatially regulated. Consistently, Mauriello *et al* (2010) found that a partially active MglA–YFP protein localizes to the leading pole. We generated an active YFP–MglA$^+$ protein, which corrected the motility defects caused by the *mglA9* mutation (Table Ic) or a Δ*mglA* mutation (data not shown). Immunoblots showed that YFP–MglA$^+$ accumulated at levels similar to MglA$^+$ in wt cells (Supplementary Figure S2). Degradation products similar in sizes to those of MglA$^+$ and YFP also accumulated, suggesting that a fraction of YFP–MglA$^+$ is cleaved near the fusion site. In moving cells, YFP–MglA$^+$ localized in a cluster at the leading pole as well as diffusely to the cytoplasm (Figure 2A). This localization is in agreement with that observed using a partially active MglA–YFP protein except that we did not observe YFP–MglA$^+$ localizing to focal adhesion complexes (Mauriello *et al*, 2010). We speculate that this difference could be caused by the partial activity of the MglA–YFP fusion used by Mauriello *et al*. Alternatively, the high background fluorescence observed with our YFP–MglA$^+$ fusion, which might be caused by degradation of the fusion protein, masks the signal from the focal adhesion complexes. YFP–MglA$^+$ localization did not change, whereas a cell was moving uni-directionally (Figure 2A). However, in reversing cells (Figure 2B), YFP–MglA$^+$ localized dynamically: 3–4 min before a reversal, the fluorescence signal at the leading pole decreased and the cytoplasmic signal increased (Figure 2B″); subsequently, YFP–MglA$^+$ accumulated at the lagging pole (Figure 2B′–B″). Once the YFP–MglA$^+$ cluster had formed at the old lagging pole, a cellular reversal occurred (Figure 2B′–B″). This dynamic YFP–MglA$^+$ localization was also observed during reversals in the presence of 25 $\mu g\ ml^{-1}$ of the translation inhibitor chloramphenicol (data not shown). We conclude that YFP–MglA$^+$ localization is dynamic. In all cells observed, the pole-to-pole relocation of YFP–MglA$^+$ occurred within a 3–4 min interval and was initiated 3–4 min before a reversal and with the actual reversal, that is the change in the direction of movement, correlating with accumulation of YFP–MglA$^+$ at the old lagging pole. A reversal occurs in two steps, first a cell stops for seconds to minutes and then the cell reverses. Depending on the duration of a stop, YFP–MglA$^+$ relocation coincides partially or fully with the stop. We conclude that YFP–MglA$^+$ localization correlates with uni-directional movement (leading pole cluster) and reversals (completion of transfer between poles).

Nucleotide-bound state regulates MglA localization

To test whether the nucleotide-bound state of MglA is critical for localization, we generated strains synthesizing YFP–MglA^{G21V} or YFP–MglA$^{T26/27N}$ at native levels (Supplementary Figure S2) as described for YFP–MglA$^+$. The mutant MglA proteins fused to YFP exhibited the same characteristics as the mutant proteins without YFP (Table Ic). Moving cells containing YFP–MglA^{G21V} (Figure 2C) reversed in a highly regular manner approximately every 4 min. YFP–MglA^{G21V} formed a cluster that was continuously and regularly oscillating from the leading towards the lagging pole with a velocity

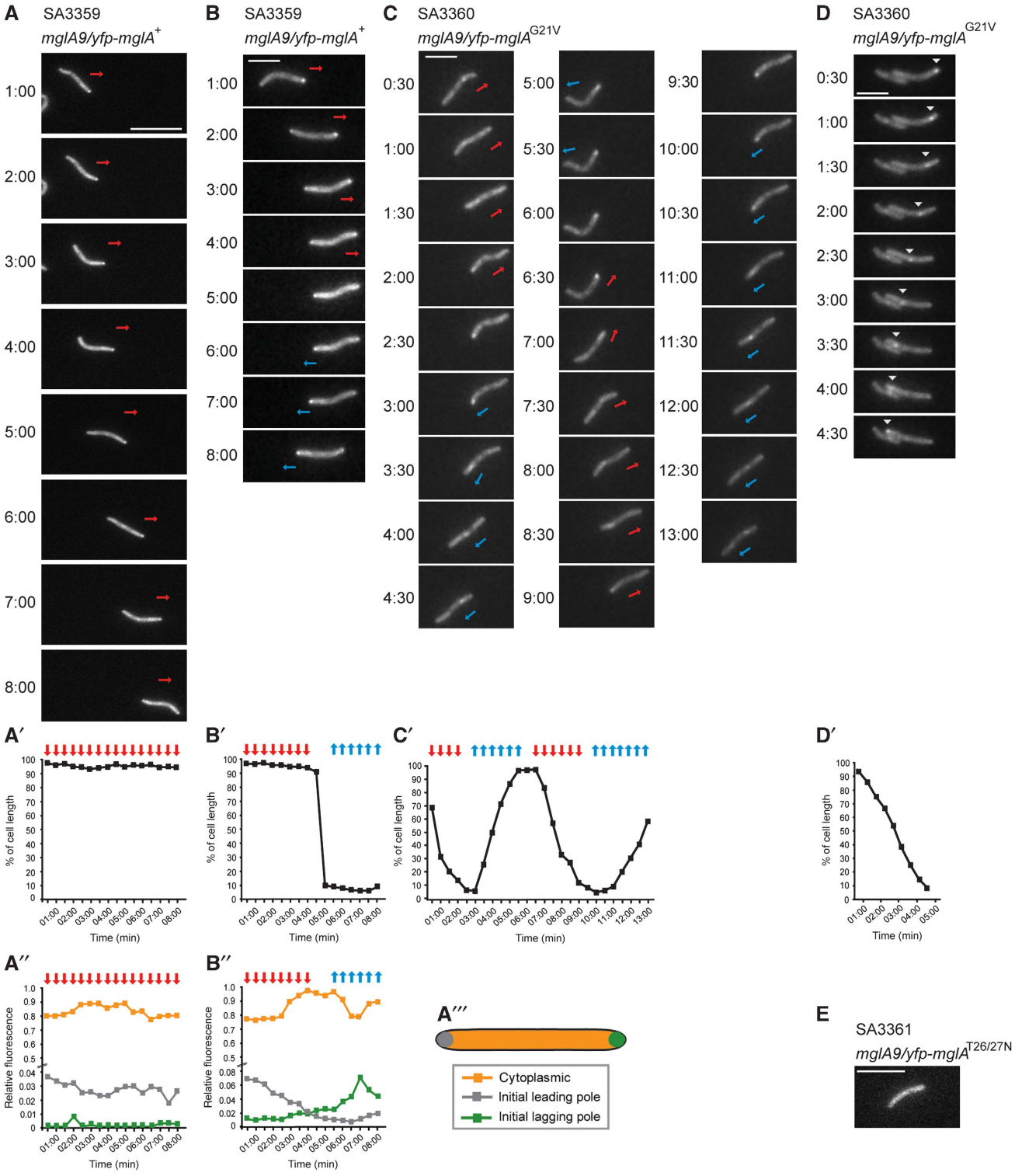

Figure 2 Correlation between MglA localization and cellular behaviour. (**A**–**E**) Cells were transferred from exponentially growing cultures to a thin agar pad on a microscope slide, and imaged by time-lapse fluorescence microscopy at 30 s intervals. Red and blue arrows indicate opposite directions of movement. Time in minutes after initiation of the recordings is shown to the left. (**A′**–**D′**) The position of the maximum fluorescence signal in the corresponding cell as percentage of cell length is plotted as a function of time. (**A″**–**B″**) Quantitative analyses of the fluorescence signals in the corresponding cell over time. Relative integrated fluorescence intensities (arbitrary units) of the polar clusters and the cytoplasmic signal were plotted as function of time. For the colour code see **A‴**. (**A‴**) Schematic indicating the three regions for which fluorescence signals were quantified. (**A**) YFP–MglA^{+} localizes in a cluster at the leading pole between reversals. Fluorescence images are shown of a representative non-reversing cell. Scale bar: 10 μm. (**B**) YFP–MglA^{+} initiates relocation between the poles before a reversal. Images are shown of a cell that reversed once. Scale bar: 5 μm. (**C**) YFP–MglA^{G21V} continuously oscillates between cell poles. Images are shown of a cell that reversed three times. (**D**) YFP–MglA^{G21V} relocates between cell poles. Fluorescence images are shown of a stalled cell. White arrows indicate the YFP–MglA^{G21V} cluster in the upper, stalled cell. Scale bar: 5 μm. (**E**) YFP–MglA$^{T26/27N}$ is diffusely localized. Scale bar: 5 μm.

of $1.3 \pm 0.2\,\mu m\,min^{-1}$, each 'arrival' of the cluster at the lagging cell pole correlating with reversal. Remarkably, after 'arriving' at the lagging pole, the YFP–MglA^{G21V} cluster immediately initiated the relocation towards the new lagging pole. Thus, in contrast to YFP–MglA^{+}, YFP–MglA^{G21V} did not form a stationary cluster at the leading pole, but continuously oscillated between the poles with a half-period of approximately 4 min. Inspection of YFP–MglA^{G21V} localization in stalled cells (Figure 2D–D′) verified that the YFP–MglA^{G21V} cluster relocated from pole-to-pole within a 4 min interval as opposed to remaining at a fixed position within a cell while the cell was moving.

The YFP–MglA$^{T26/27N}$ fluorescence signal was homogenously distributed throughout the cytoplasm (Figure 2E). The signal failed to segregate to the poles and localization did not change over time. The localization, the biochemical characteristics, and the *in vivo* activities of the three MglA proteins suggest that MglA localizing in a cluster at the leading pole as well as relocating MglA is MglA in the GTP-bound state and that the inactive form localizes diffusely to the cytoplasm.

Frz chemosensory system induces relocation of MglA

As MglA acts downstream of Frz to induce reversals and the accumulation of MglA in a cluster at the old lagging pole correlates with reversal, we hypothesized that Frz stimulates the dynamic localization of MglA. To test this idea, we analysed the localization of YFP–MglA^{+} and YFP–MglA^{G21V} in *frz*^{lof} and *frz*^{gof} mutants. In the non-reversing *frz*^{lof} mutant, YFP–MglA^{+} localized in a cluster at the leading pole and did not display dynamic localization (Figure 3A). In the hyper-reversing *frz*^{gof} mutant, YFP–MglA^{+} also accumulated in a cluster at the leading pole between reversals, and during the frequent reversals, the cluster relocated between the poles (Figure 3B–B′). In the *frz*^{lof} mutant, the same localization pattern of YFP–MglA^{G21V} was observed as in the *frz*$^{+}$ strain and with YFP–MglA^{G21V} forming a cluster that oscillated regularly between the poles with a 4 min half-period, each 'arrival' of the cluster at the lagging pole correlating with reversal (Figure 3C–C′; cf. Figure 1C′). A similar localization of YFP–MglA^{G21V} was observed in the *frz*^{gof} mutant (data not shown). Thus, the Frz system is not necessary for polar localization of MglA^{+}, but it is necessary and sufficient for

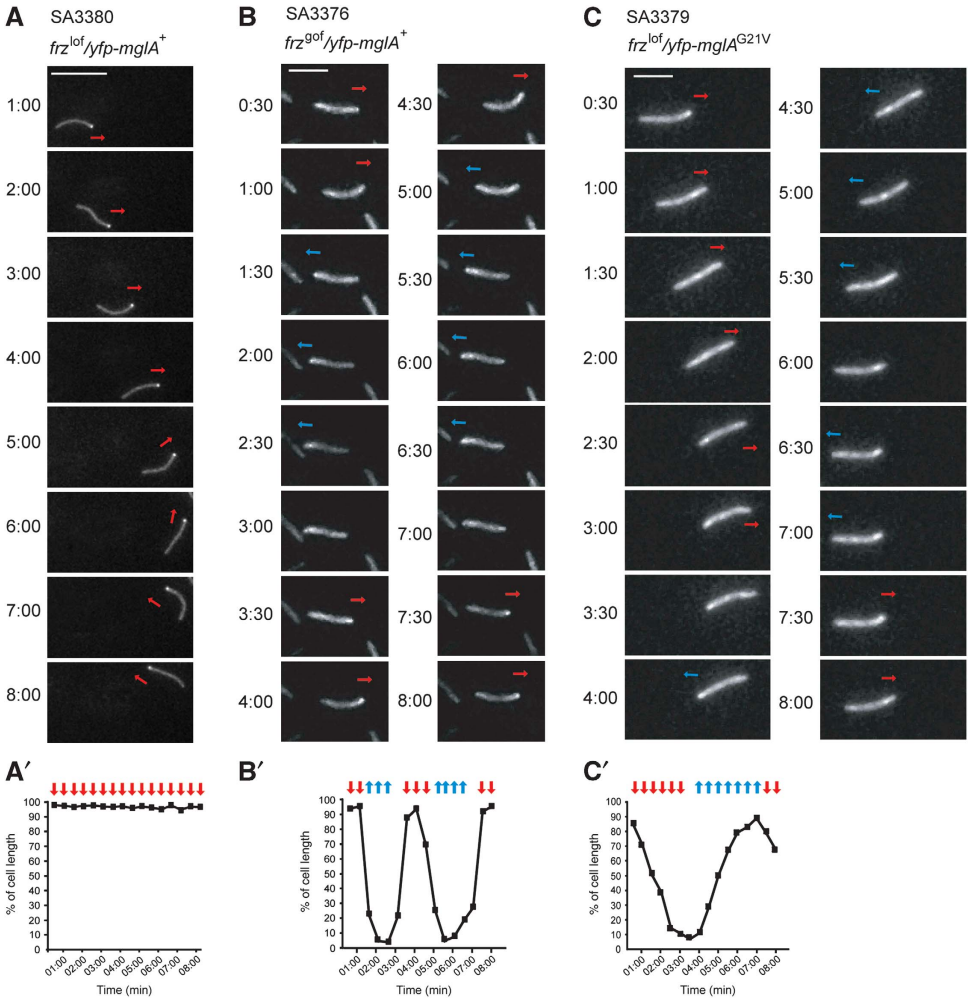

Figure 3 Dynamic localization of MglA is regulated by the Frz system. (**A**–**C**) Cells were treated as in Figure 2. Red and blue arrows indicate opposite directions of movement. Time in minutes after initiation of the recordings is shown to the left. (**A**′–**C**′) The position of the maximum fluorescence signal in the corresponding cell as percentage of cell length is plotted as a function of time. (**A**) The Frz system is required for dynamic YFP–MglA^{+} localization. Images are shown of a representative non-reversing cell. Scale bar: 10 μm. (**B**) The Frz system is sufficient for dynamic YFP–MglA^{+} localization. Scale bar: 4 μm. (**C**) YFP–MglA^{G21V} bypasses a *frz*^{lof} mutation with respect to reversals. Images are shown of a cell that reversed three times. Scale bar: 5 μm.

pole-to-pole relocation of MglA$^+$ during reversals. The two separable activities of MglA, their differential dependency on Frz, and the localization patterns of the mutant MglA proteins suggest that Frz by further stimulating accumulation of MglA/GTP induces the release of MglA/GTP from the leading pole and the subsequent relocation towards the lagging pole.

MglB regulates MglA activity and localization

To examine whether MglB is involved in the regulation of MglA activity, we generated a Δ*mglB* mutant. This mutant accumulated normal levels of MglA (data not shown) and moved with normal velocity, but reversed two-fold more frequently than wt (Table Id). Furthermore, a fully active MglB–YFP protein (Table Id) accumulating at a level similar to that of MglB in wt cells (Supplementary Figure S3) localized in a cluster at the lagging pole in cells moving uni-directionally (Figure 4A). In reversing cells, the MglB–YFP cluster relocated from the old lagging to the new lagging cell pole in parallel with a cellular reversal (Figure 4B). In contrast to YFP–MglA$^+$ (Figure 2B″), this relocation occurred during the reversal (Figure 4B″). Dynamic MglB–YFP localization was also observed during reversals in the presence of 25 μg ml^{-1} chloramphenicol (data not shown). Thus, MglB–YFP localization is dynamic during reversals, but relocation is initiated significantly later than in the case of MglA$^+$.

To test whether MglA is involved in MglB localization, we analysed MglB–YFP in a Δ*mglA* mutant. In these non-moving cells ($N = 100$), 84% contained MglB–YFP in bipolar, symmetric clusters and 16% contained a single MglB–YFP cluster (Figure 4C). Thus, compared with the localization of MglB–YFP in stalled *mglA*$^+$ cells, MglB–YFP localization was shifted from a unipolar to a bipolar and symmetric pattern in the Δ*mglA* cells. Next, we analysed YFP–MglA$^+$ localization in the Δ*mglB* mutant. In this mutant, YFP–MglA$^+$ formed essentially symmetric and bipolar clusters (Figure 4D–D″) and generally with the larger cluster at the leading pole (Figure 4D′). Moreover, the larger YFP–MglA$^+$ cluster relocated between the poles during reversals (Figure 4D′–D″).

Localization of MglA in the absence of MglB and MglB in the absence of MglA is shifted towards bipolar and symmetric suggesting that a mutually exclusive mechanism maintains MglA and MglB at opposite poles. As our data suggest that MglA localizing in a cluster at the leading pole is MglA/GTP and that the inactive form localizes diffusely to the cytoplasm, one mechanism by which MglB could inhibit MglA accumulation at the lagging pole would be to act as an MglAGAP.

To determine biochemically the function of MglB, we initially tested whether MglB is a nucleotide-binding protein and found that MglB neither binds mGDP/mGTP nor mADP/mATP (data not shown). The binding between a Ras-like G-protein and an interaction partner can be measured using fluorescent changes of mant-labelled nucleotides as shown for Ras and its GAP neurofibromin (Mittal *et al*, 1996; Ahmadian *et al*, 1997; Gremer *et al*, 2008) or Arl3 and its GAP RP2 (Veltel *et al*, 2008). A significant increase in fluorescence polarization was obtained on titrating MglB to MglA$^+$/mGppNHp, but not to MglA$^+$/mGDP (Figure 5A). The affinity to MglA$^+$/mGppNHp was 60-fold higher (Figure 5A) compared with MglA$^+$/GDP strongly suggesting that MglB senses and specifically binds to the active, GTP-bound conformation of MglA.

Ras-like proteins with bound GDP bind the transition state analogue aluminium fluoride (AlF_x) only in the presence of a GAP (Mittal *et al*, 1996; Daumke *et al*, 2004; Gremer *et al*, 2008; Veltel *et al*, 2008). We used two approaches to test whether MglB can form a complex with MglA$^+$/GDP in the presence of AlF_x, as this can be considered the litmus test of whether a protein acts as a GAP (Gasper *et al*, 2009). First, as shown in Figure 5A, a significant increase in the polarization signal was detected with MglA$^+$/mGDP in the presence of AlF_x and MglB. Second, using size exclusion chromatography, we found that MglA$^+$ elutes as a monomer at an elution volume corresponding to an apparent molecular mass of 22 kDa irrespective of the nucleotide-bound state, whereas MglB (17 kDa) elutes at a volume suggesting that it is a dimer or tetramer (Figure 5B, upper panel). No complex formation between MglB and MglA$^+$ in its GDP-bound conformation was observed (Figure 5B; lower panel). However, addition of AlF_x to this mixture resulted in complex formation as the proteins co-eluted in a single peak. Likewise, MglA$^+$ in its mGppNHp-bound conformation co-eluted with MglB (Figure 5B, lower panel). These results strongly suggest that MglB is MglA's cognate GAP and has the capability of stabilizing the transition state of the GTPase reaction.

The GTPase reaction of a Ras-like G-protein is usually very slow and is accelerated in the presence of its cognate GAP, for example the slow intrinsic GTPase reaction of Ras is accelerated approximately 10^5-fold by RasGAP (Ahmadian *et al*, 1997), as is the GTPase activity of Rap by its cognate RapGAP (Daumke *et al*, 2004). To test whether MglB accelerates the GTPase reaction of MglA, we analysed GTP hydrolysis in the presence and absence of MglB. The slow intrinsic GTP-hydrolysis rate of MglA$^+$ of 0.00009 s^{-1} was accelerated by catalytic amounts of MglB to 0.00027 s^{-1} and more than 100-fold by stoichiometric amounts of MglB (Figure 5C), confirming that MglB is an MglAGAP. In contrast, MglA^{G21V} and MglA$^{T26/27N}$ showed no measurable GAP-stimulated GTP-hydrolysis with catalytic amounts of MglB (Figure 5C) and only a slight increase with stoichiometric amounts of MglB (data not shown). Moreover, binding of MglB to MglA^{G21V} and MglA$^{T26/27N}$ in their active, GTP-bound conformation could still be detected (data not shown). Thus, we conclude that the substitutions in MglA inhibit the MglB-stimulated GTP hydrolysis rather than MglB binding showing the similarity to the Ras–RasGAP system, in which the G12V substitution inhibits GAP-mediated GTP hydrolysis, but not GAP binding (Gremer *et al*, 2008).

MglA regulates the polarity of motility proteins

The earlier analyses suggested that MglA activity is temporally and spatially regulated by Frz and MglB. To identify downstream targets of MglA, we examined whether MglA activity has a function in the localization of three motility proteins, RomR, AglZ, and PilT.

In *mglA*$^+$ cells, RomR–GFP localizes with a large cluster at the lagging pole and a small cluster at the leading pole (Figure 6A; Supplementary Figure S4). In parallel with a reversal, the large RomR–GFP cluster relocates from the old lagging to the new lagging pole. In the *mglA*^{G21V} mutant, RomR–GFP localized in a bipolar, symmetric pattern (Figure 6B; Supplementary Figure S4). Moreover, during the frequent reversals, the symmetric localization of RomR–GFP did not change. In the *mglA*$^{T26/27N}$ mutant ($N = 100$),

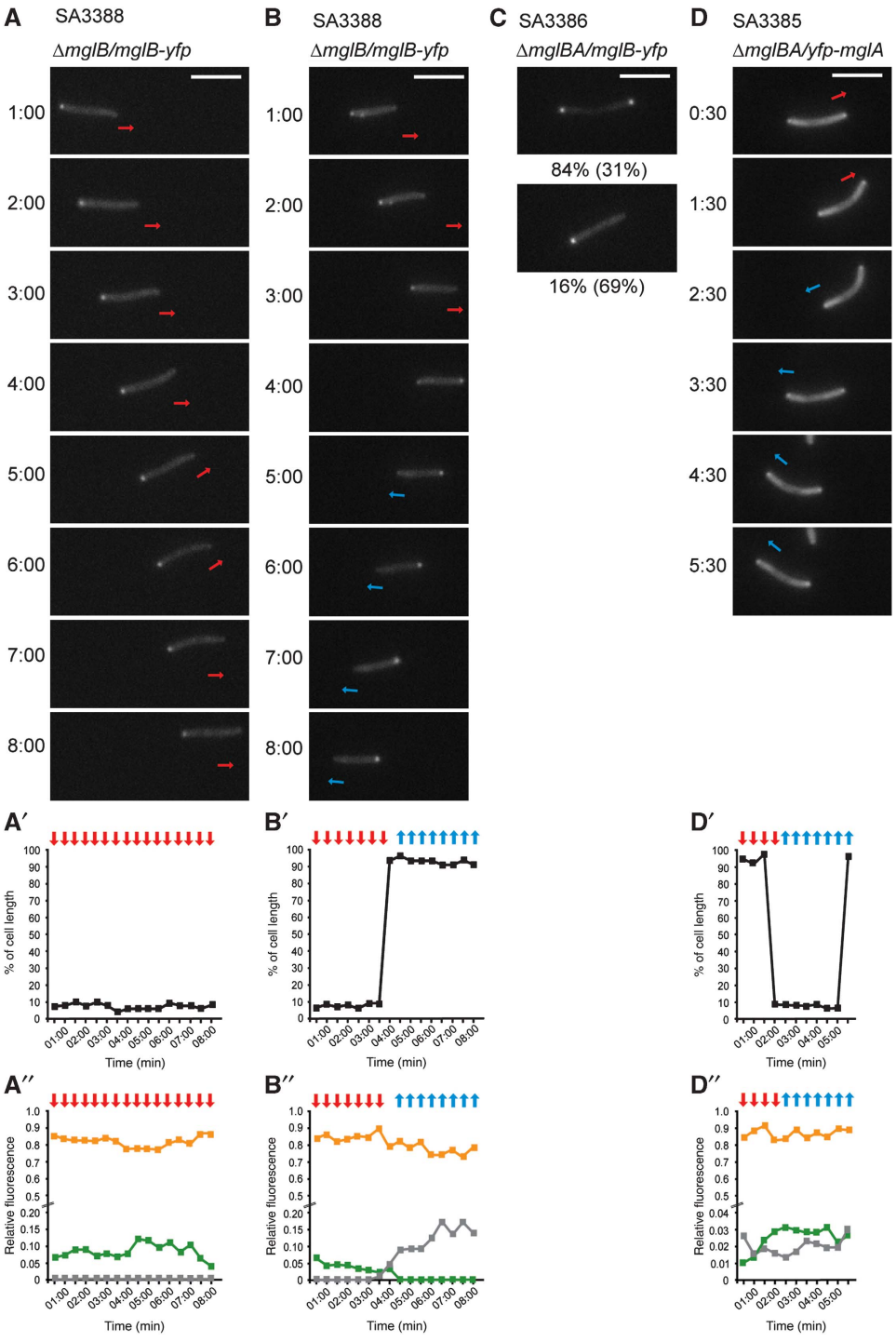

Figure 4 MglB is localized to the lagging pole and dynamic during reversals. (**A**, **B**, **D**) Cells were treated as in Figure 2. Red and blue arrows indicate opposite directions of movement. Time in minutes after initiation of the recordings is shown to the left. (**A′**, **B′**, **D′**) The position of the maximum fluorescence signal in the corresponding cell as percentage of cell length is plotted as a function of time. (**A″**, **B″**, **D″**) Quantitative analyses of the fluorescence signals in the corresponding cell over time. Relative integrated fluorescence intensities (arbitrary units) of the polar clusters and the cytoplasmic signal were plotted as function of time. For the colour code see Figure 2A‴. (**A**) MglB–YFP localizes in a cluster at the lagging pole between reversals. Images are shown of a representative non-reversing cell. Scale bar: 5 μm. (**B**) MglB–YFP relocates between the poles during a reversal. Images are shown of a cell that reversed once. Scale bar: 5 μm. (**C**) In the absence of MglA, MglB–YFP localizes symmetrically at both poles. Images are shown of two cells that did not move. The percentage of cells with unipolar or bipolar symmetric localization of MglB–YFP are shown. Numbers in brackets indicate the same percentages in stalled *mglA*$^+$ cells. Scale bar: 5 μm. (**D**) MglB regulates YFP–MglA$^+$ localization. Images are shown of a cell that reversed once. Scale bar: 5 μm.

RomR–GFP failed to localize at both poles. Rather in 86% of cells, RomR–GFP localized only at one pole. By staining of T4P, this pole was identified as the pole containing T4P, that is the 'wrong' pole (Figure 6C), whereas the remaining 14% had RomR–GFP at the 'correct' pole. In addition, RomR–GFP did not relocate between the poles in this mutant. Thus,

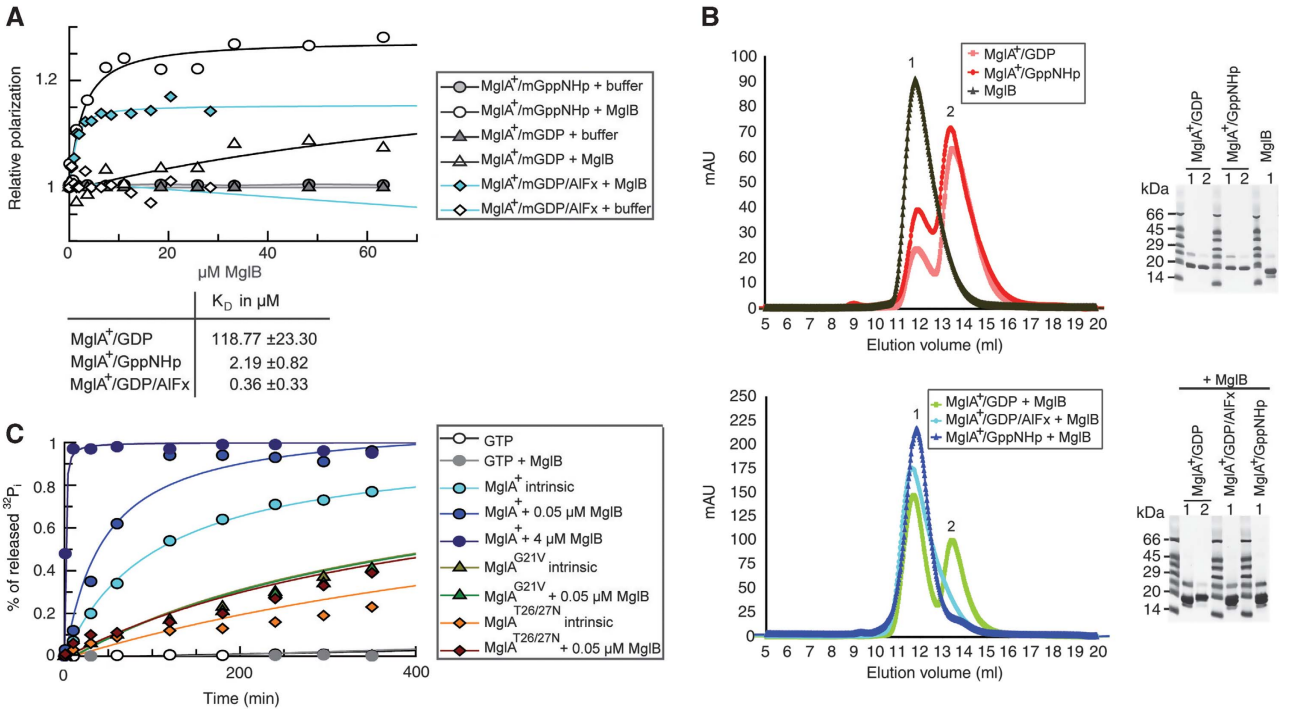

Figure 5 MglA is a Ras-like G-protein and MglB a MglAGAP. (**A**) MglB binds to MglA$^+$ in its active GTP-bound form (MglA$^+$/mGppNHp) and to MglA$^+$/GDP in the presence of AlF_x. The K_d for binding of MglB to 1 μM MglA$^+$ containing mGDP, mGppNHp, or mGDP/AlF_x is indicated below the graph and was determined by measuring the relative polarization during titration of MglB. (**B**) MglB stabilizes the transition state of GTP-hydrolysis mimicked by AlF_x. Shown are elution profiles from analytic gel filtration. Upper panel, elution profile of MglB and MglA$^+$ bound to GDP and GppNHp, respectively. Lower panel, elution profile after mixing MglB with MglA$^+$ bound to GDP, GppNHp, or GDP/AlF_x. On the right side, the corresponding SDS–PAGE are shown of aliquots of the peak maxima (indicated with 1 and 2). (**C**) MglB stimulates the intrinsic GTPase activity of MglA$^+$ and MglA mutants have lost MglB-stimulated GTP hydrolysis. Graph depicts the release of $^{32}P_i$ using the charcoal assay in the presence of 4 μM of MglA$^+$, MglA^{G21V}, and MglA$^{T26/27N}$ bound to 60 nM [γ-^{32}P]GTP with and without the addition of 0.05 or 4 μM MglB as indicated.

MglA activity is important for establishing correct RomR polarity.

AglZ–YFP localizes in a large cluster at the leading pole and in small clusters along the cell body in *mglA*$^+$ cells (Figure 6D; Supplementary Figure S5). In parallel with a reversal, the polar AglZ–YFP cluster relocated. In *mglA*^{G21V} cells, AglZ–YFP localized as in *mglA*$^+$ cells and the frequent reversals were accompanied by relocation of the large cluster (Figure 6E; Supplementary Figure S5). In the non-moving *mglA*$^{T26/27N}$ cells ($N = 100$), 69% of cells displayed a homogeneous distribution of AglZ–YFP, 31% contained AglZ–YFP in a cluster at one pole, and no cells contained small clusters along the cell body (Figure 6F). This distribution is similar to the localization of AglZ–YFP in stalled wt cells (cf. Figure 6F). To resolve at which pole AglZ–YFP localizes in *mglA*$^{T26/27N}$ cells, we attempted to co-visualize T4P and AglZ–YFP in the same cells. However, under the conditions used for visualizing T4P, AglZ–YFP fails to localize to a pole (data not shown). Therefore, we co-visualized AglZ–GFP together with RomR–mDsRed in the same cells. In *mglA*$^+$ cells, RomR–DsRed and AglZ–YFP localized to opposite pole, whereas in *mglA*$^{T26/27N}$ cells both proteins localized to the same pole (Figure 6G). Therefore, AglZ–YFP localizes correctly at the pole containing T4P in the *mglA*$^{T26/27N}$ mutant. Thus, MglA activity is not important for establishing correct AglZ polarity, but MglA regulates the dynamic localization of AglZ.

YFP–PilT localized with a large cluster at the lagging pole (Figure 6H; Supplementary Figure S6) and with a small cluster occasionally accumulating at the leading pole in *mglA*$^+$ cells. In parallel with a reversal, the large YFP–PilT cluster relocated. In *mglA*^{G21V} cells, YFP–PilT localized as in *mglA*$^+$ cells and the frequent reversals were accompanied by relocation of the large YFP–PilT cluster (Figure 6I; Supplementary Figure S6). In the non-moving *mglA*$^{T26/27N}$ cells ($N = 100$), YFP–PilT localization was shifted to a more unipolar pattern compared with the bipolar, symmetric pattern in stalled *mglA*$^+$ cells (Figure 6J). By staining of T4P, this pole was identified as the pole not containing T4P (data not shown). Thus, MglA activity is important for establishing correct PilT polarity and MglA regulates dynamic localization of PilT.

Discussion

In this study, we provide evidence that MglA is a Ras-like G-protein that functions as a nucleotide-dependent molecular switch to establish the correct polarity of motility proteins and to inverse their polarity during cellular reversals. Moreover, we show that MglA activity is regulated spatially and temporally by the MglAGAP MglB and the Frz system. According to the eukaryotic paradigm for Ras-like proteins, these proteins interact with three types of proteins: GEF and GAP, which have regulatory functions, and effectors that are components of downstream pathways involved in eliciting a particular response. Below we discuss our findings within the framework of this paradigm.

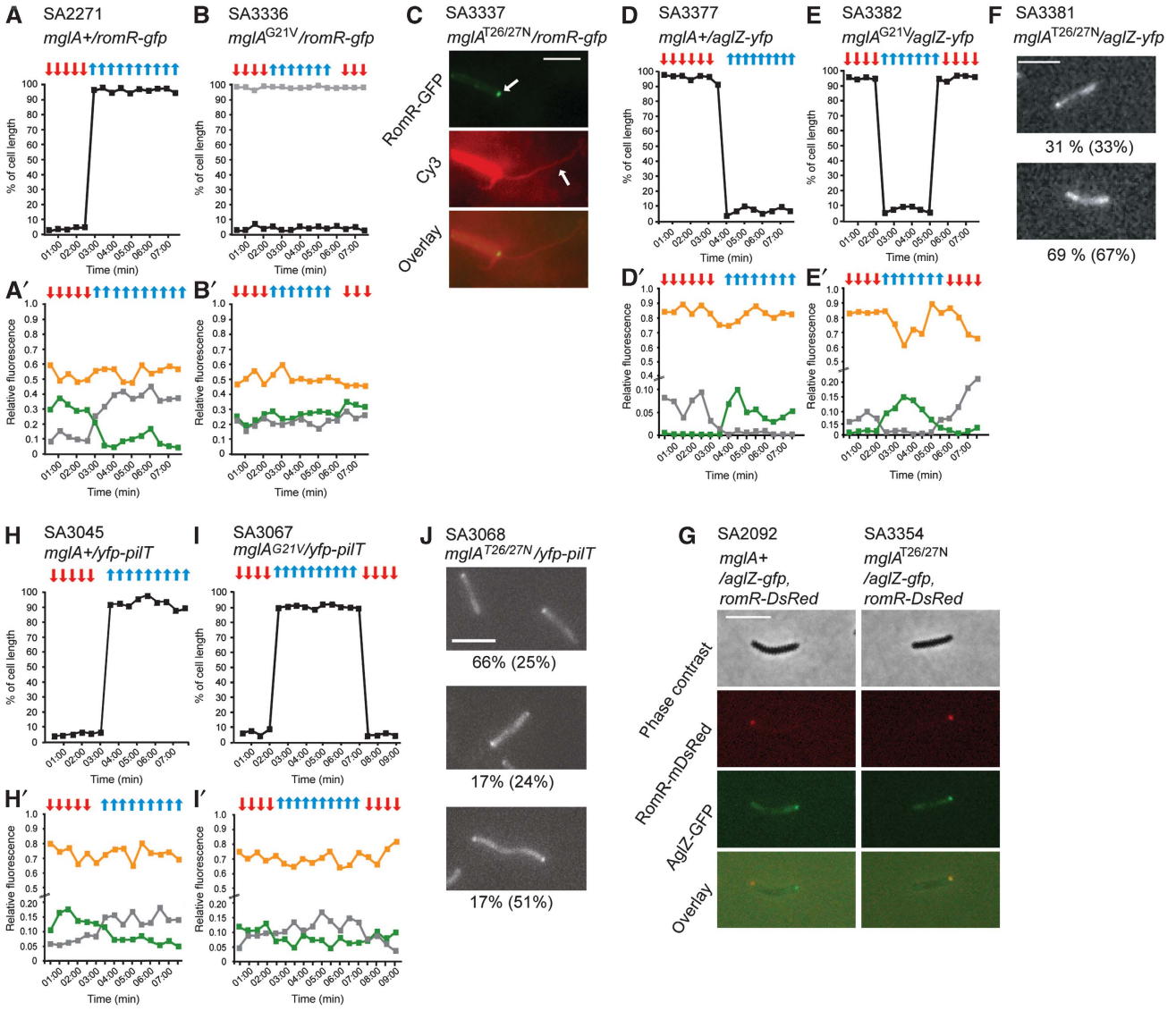

Figure 6 MglA activity establishes correct polarity and regulates dynamic localization of motility proteins. (**A–B**, **D–E**, **H–I**) Cells were treated as in Figure 2. The position of the maximum fluorescence signal of the cells shown in Supplementary Figure S4A and B (**A–B**), Supplementary Figure S5A and B (**D–E**), and Supplementary Figure S6A and B (**H–I**) as percentage of cell length is plotted as a function of time. (**A′–B′**, **D′–E′**, **H′–I′**) Quantitative analyses of the fluorescence signals in the same cells over time. Relative integrated fluorescence intensities (arbitrary units) of the polar clusters and the cytoplasmic signal were plotted as function of time. For the colour code see Figure 2A‴. Red and blue arrows indicate opposite directions of movement. (**A**) RomR–GFP localization is bipolar, asymmetric between reversals and dynamic during reversals in MglA^{+} cells. (**B**) MglA^{G21V} changes RomR–GFP polarity. (**C**) MglA$^{T26/27N}$ is unable to establish correct RomR–GFP polarity. Cells of SA3337 were grown on 1.5% agar plates supplemented with 1% CTT, scraped off the agar stained with Cy3 to visualize T4P and inspected by fluorescence microscopy (Cy3, white arrow) and RomR–GFP (GFP, white arrow). Lower panel is the overlay of the fluorescence images. Scale bar: 5 μm. (**D**) AglZ–YFP localizes in a cluster at the leading pole and is dynamic during reversals. (**E**) MglA^{G21V} regulates dynamic AglZ–YFP localization. (**F**) MglA$^{T26/27N}$ does not interfere with correct AglZ–YFP polarity. The percentage of cells with unipolar or diffuse localization of AglZ–YFP are shown. Numbers in brackets indicate the same percentages in stalled *mglA*$^{+}$ cells. Scale bar: 5 μm. (**G**) Opposite polarity of RomR–mDsRed and AglZ–YFP is absent in *mglA*$^{T26/27N}$ mutant. Cells were treated as in (**A–B**, **D–E**, **H–I**). Shown are phase-contrast and fluorescence images as well as the overlays of the fluorescence and phase-contrast images. Scale bar: 4 μm. (**H**) YFP–PilT localizes in a large cluster at the lagging pole and localization is dynamic during reversals. (**I**) MglA^{G21V} regulates dynamic YFP–PilT localization. (**J**) MglA$^{T26/27N}$ is unable to establish correct YFP–PilT polarity. The percentage of cells with unipolar, bipolar, asymmetric or bipolar, symmetric localization of YFP–PilT are shown. Numbers in brackets indicate the same percentages in stalled *mglA*$^{+}$ cells. Scale bar: 4 μm.

MglA is a molecular switch that stimulates motility and cellular reversals

Genetic analyses showed that MglA/GTP represents the active form of MglA, suggesting that as in other G-proteins, MglA/GDP is the inactive form. MglA/GTP has two activities, stimulation of motility and stimulation of reversals. Two lines of evidence establish a link between MglA/GTP levels and MglA/GTP function. First, we directly showed that MglB functions as an MglAGAP, which converts the active MglA/GTP to inactive MglA/GDP, and an *mglB* mutant, which is predicted to accumulate increased amounts of MglA/GTP, moves with a normal velocity, but reverses more frequently than *mglB*$^{+}$ cells. Second, the mutant protein MglA^{G21V}, which is locked in the GTP-bound form, stimulates motility

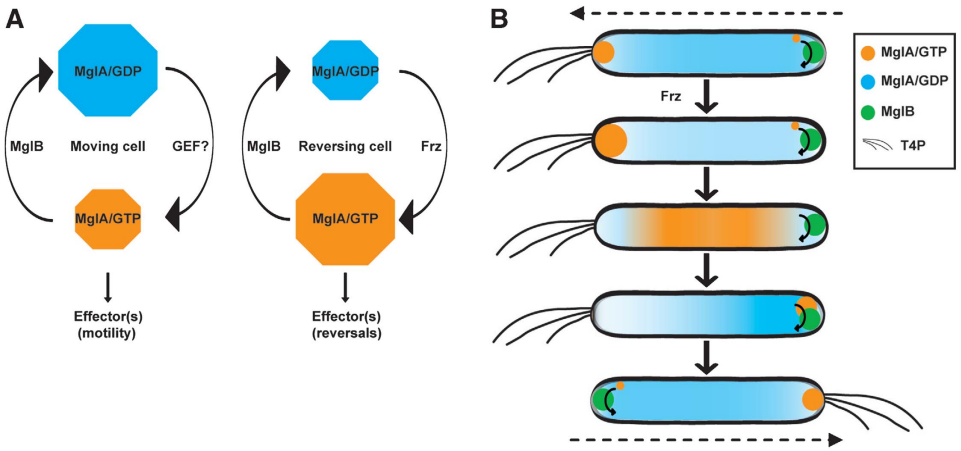

Figure 7 Model of temporal and spatial regulation of MglA activity. (**A**) Temporal regulation of the nucleotide-bound state of MglA. In moving cells, MglA/GTP is present in a low concentration and interacts with effector(s) to stimulate motility. Before a reversal, Frz activity—directly or indirectly—stimulates MglA/GTP accumulation. At the increased concentration, MglA/GTP interacts with effector(s) that stimulate reversals. These effector(s) likely include proteins involved in relocation of MglA and motility proteins. (**B**) MglA/GTP and MglB set up the leading/lagging polarity axis. In moving cells (upper panel), this axis is stably maintained with the two proteins at opposite poles. At the lagging pole, MglB likely excludes MglA by converting MglA/GTP to MglA/GDP (arrow). In response to Frz activity (second panel), MglA/GTP accumulation is further stimulated at the leading pole followed by release and relocation to the lagging pole (third panel). Here, MglA/GTP interacts shortly with the MglAGAP MglB resulting in a reduction in the MglA/GTP concentration and MglA/GTP binding at the pole (fourth panel). Simultaneously, MglB is excluded from this pole and relocates to the opposite pole (fifth panel). Dashed arrows indicate direction of cell movement.

normally, but bypasses the requirement for Frz for reversals. On the basis of these observations, we propose that MglA/GTP functions in a concentration-dependent manner and that a low concentration of MglA/GTP stimulates motility and a high concentration stimulates reversals (Figure 7A).

MglA activity is temporally and spatially regulated by Frz and MglB

By analysing the localization of three MglA proteins, we established a direct link between MglA/GTP localization and function. Between reversals, MglA/GTP localizes to a cluster at the leading pole, whereas the inactive form localizes diffusely to the cytoplasm. Several minutes before a reversal and in response to Frz activity, MglA/GTP is released from the leading pole and relocates to the lagging pole. On accumulation of MglA/GTP at the lagging pole, a reversal is induced. Together with our genetic analyses, these findings suggest that Frz activity further stimulates MglA/GTP accumulation at the leading pole. Once a threshold is reached, MglA/GTP is released from this pole.

Although the primary function of Frz is to induce the relocation of MglA, the primary function of MglB is in establishing spatial MglA/GTP asymmetry. Between reversals, MglA/GTP and MglB localize to opposite poles. However, each protein localizes in a bipolar and symmetric pattern in the absence of the other suggesting that the localization at opposite poles depends on a mutually exclusive mechanism. As we directly showed that MglB has MglAGAP activity, MglB likely excludes MglA/GTP from the lagging pole between reversals by locally converting MglA/GTP to MglA/GDP. How MglA/GTP excludes MglB from the leading pole remains to be clarified.

During reversals, the polarity of MglA/GTP and MglB is inverted. MglA/GTP relocation from the leading pole is initiated several minutes before a reversal (cf. Figure 2B), whereas MglB relocation from the lagging pole is initiated during the reversal (cf. Figure 4B). We infer that during a reversal, MglA/GTP 'arriving' at the lagging pole at a high concentration interacts briefly with MglB causing a stimulation of MglA GTPase activity. As this results in a decrease in the MglA/GTP concentration, MglA/GTP can form a cluster at this pole. In parallel—and by an unknown mechanism—MglA/GTP excludes MglB from this pole causing its relocation to the new lagging pole. On the basis of the data showing that MglB is an MglAGAP at the lagging pole and that MglA/GTP relocation is initiated earlier than in the case of MglB, we suggest that the output of the Frz system is to directly or indirectly act as a GEF at the leading pole by converting MglA/GDP in a cytoplasmic pool to MglA/GTP. In current models of the Frz system, the output is the phosphorylated response regulator FrzZ (Inclan *et al*, 2007). We have been unable to detect direct interactions between MglA proteins or MglB and FrzZ, respectively (data not shown). Likewise, we have been unable to detect specific localization of FrzZ∼P (data not shown). Although these results are all negative, they indicate that FrzZ∼P may not act directly on MglA/GDP, but indirectly by stimulating an unknown GEF.

In total, we suggest that at the core of the regulatory circuit that sets up the leading/lagging polarity axis with MglA at the leading pole and MglB at the lagging pole is the mutually exclusive localization of MglA/GTP and MglB (Figure 7B). The series of events set in motion by Frz activity results in inversion of the leading/lagging polarity axis, and as a consequence, a cellular reversal ensues. Thus, the mutually exclusive localization of MglA and MglB sets up a stable polarity axis, which can be dynamically inverted in response to Frz activity. The asymmetric distribution of MglA and its cognate GAP is similar to that observed in eukaryotic systems involved in regulation of cell polarity, for example in the regulation of Ras by RasGAP in *D. discoideum* (Zhang *et al*,

2008), Cdc42 by Rga1 in *S. cerevisiae* (Tong *et al*, 2007) and Rho by RhoGAP in *Caenorhabditis elegans* (Anderson *et al*, 2008). Interestingly, in the latter case, this asymmetry also depends on a mutually exclusive mechanism. Although our model explains the basic circuit underlying the leading/lagging polarity axis and how it can be inverted, there are several unresolved questions. For instance, how does MglA/GTP exclude MglB from the leading pole? How does polar and dynamic MglA/GTP localization depend on concentration? What are the molecular nature of the landmarks recognized by MglA and MglB at the cell poles? Likewise, we do not know whether there is a GEF acting on MglA/GDP that regulate the accumulation of MglA/GTP between reversals. We are currently addressing these questions experimentally.

MglA establishes correct polarity of motility proteins and regulates their dynamic localization

Analyses of the order of events during the pole-to-pole relocation of AglZ, FrzS, PilT, and RomR have shown that completion of relocation of the large polar clusters coincides with the reversal. The early release of MglA and the late release of AglZ, FrzS, PilT, and RomR suggested that MglA regulates the localization of motility proteins. Consistently, we found that MglA activity is required to establish the correct polarity of RomR and PilT, whereas correct AglZ polarity is established independently of MglA. This was a surprising observation given that AglZ and MglA interact directly (Yang *et al*, 2004; Mauriello *et al*, 2010). MglA locked in GTP-bound state induces frequent pole-to-pole relocation of AglZ and PilT and loss of asymmetric RomR localization. These data suggest that the two separable functions of MglA, that is stimulation of motility and stimulation of reversals, are manifested in these two distinct activities, establishment of polarity of some motility proteins and regulation of their dynamic localization. Accordingly, MglA is not part of the motility machineries and not a motility protein *per se*. Rather the motility defects in Δ*mglA* and *mglA*$^{T26/27N}$ mutants are caused by incorrect localization of motility proteins. The continuous oscillations of MglA^{G21V} without the formation of a stationary cluster at the leading pole as well as the observation that MglA^{+} is released from the leading pole 3–4 min before the actual reversal and that cells continue to move in these 3–4 min support the idea that MglA is not a component of the motility machineries. The correct polarity of AglZ in the absence of MglA activity suggests that other mechanisms are also involved in establishing polarity of motility proteins. So far, the localization of five dynamically localized motility proteins has been shown to depend on Frz. We suggest that dynamic localization of motility proteins depend on MglA. Such a 'one-for-all' mechanism would ensure that once established, the correct polarity of dynamically localized proteins is maintained over time guaranteeing that the two motility systems generate force in the same direction.

We currently do not know which effectors MglA interacts with to establish the correct polarity and induce pole-to-pole relocation of motility proteins. However, our data allow some speculations. PilT and RomR both localize with a large cluster at the lagging pole. As the large MglA^{+} cluster is at the leading pole, this suggests that MglA does not establish the correct polarity of these proteins by recruiting them to the lagging pole. Likewise, the accumulation of MglA/GTP at the lagging pole during a reversal induces the relocation of proteins from the leading to the lagging pole and *vice versa*. It is difficult to imagine how this would happen by direct interactions only. Recently, Mauriello *et al* (2010) observed that AglZ and FrzS cluster formation depends on the actin-like protein MreB, which forms a helix spanning the length of a cell in *M. xanthus*. Thus, it is a possibility that MglA regulates the polarity of MreB—or some other cytoskeletal element—to direct motility proteins in a vectorial manner to the correct poles. According to this scheme, relocation of MglA could result in an inversion of the polarity of MreB—or some other cytoskeletal element—and in this way, induce an inversion of the polarity of motility proteins. In this regard, it is interesting that directed motility of eukaryotic cells requires the polarized activity of Ras-like G-proteins of the Rho subfamily, which directly regulate re-organization of the actin cytoskeleton (Etienne-Manneville, 2004; Charest and Firtel, 2007). It is also interesting to note that translocation of MglA^{+} and MglA^{G21V} from the leading to the lagging pole occurs in a highly directed manner (cf. Figure 2B–D) unlike that expected for freely diffusing molecules and on a time-scale much slower than diffusion (Bulyha *et al*, 2009). In the absence of molecular motors such as kinesin, dynein, and myosin in bacteria, this relocation dynamics suggest that a cytoskeletal element pushes or pulls MglA from the leading to the lagging cell pole.

Each of the five major eukaryotic subfamilies of Ras-like G-proteins has its own cognate GEFs and GAPs with little if any sequence homology between GEFs and GAPs of different subfamilies (Vetter and Wittinghofer, 2001; Bos *et al*, 2007). GEFs and GAPs have in common that they are usually large multidomain proteins (Bos *et al*, 2007). MglB is a small protein of 17 kDa and does not show homology to known GAPs suggesting that it represents a novel GAP family. MglB is a member of the Roadblock/LC7 protein family implicated in regulation of NTPase activity and with members in all three domains of life (Koonin and Aravind, 2000). Thus, MglB GAP activity may be widely conserved.

To our knowledge, this is the first report showing a function of a Ras-like G-protein in establishing and maintaining cell polarity in bacteria. The finding that MglA functions and is regulated in a manner that shares many—if not all—of its characteristics with its eukaryotic counterparts provides evidence that the function of this family of proteins in regulation of polarity can be extended to include bacteria. MglA and MglB orthologues are found in many phylogenetically distant bacteria and archaea (Koonin and Aravind, 2000), suggesting that regulation of polarity by a Ras-like G-protein and its cognate GAP is a general feature in bacteria.

Materials and methods

Construction of plasmids and strains, cell growth, antibody generation, immunoblot analysis, protein purification, and biochemical methods

These procedures are described in the Supplementary data. A list of strains is given in Supplementary Table SI.

Microscopy, determination of reversal period, and data analysis

For microscopy, *M. xanthus* cells were grown and treated for time-lapse microscopy as described earlier (Leonardy *et al*, 2007; Bulyha *et al*, 2009). Cells were imaged at 30 s intervals for 10 to 15 min, and images were recorded and processed with Leica FW4000 V1.2.1 or Image Pro 6.2 (MediaCybernetics) software. Processed images were

visualized in Metamorph 7.0r2 software (Molecular Devices). Quantification of fluorescence was performed as follows. Integrated fluorescence intensities (arbitrary units) of polar clusters and the cytoplasmic region between the polar clusters (Figure 2A‴) were quantified using the region measurement tool in Metamorph 7.0r2. Relative fluorescence intensities were calculated by dividing the integrated fluorescence intensities with the total fluorescent intensity of a cell. The linescan tool in Metamorph 7.0r2 was used to determine the position of the maximum fluorescence signal in a cell. This position was plotted as a function of time. T4P were visualized as described (Leonardy *et al*, 2007). To calculate reversal periods, the total number of moving cells was multiplied by the elapsed time and divided by the number of reversals. The velocity of moving cells was determined using the object track tool in Metamorph. Unless otherwise stated, 25 cells were analysed per experiment.

Nucleotide-binding assays

MglA proteins were made nucleotide free before determination of nucleotide affinities (Supplementary data). Fluorescence and polarization data were recorded with a Fluoromax-2 spectrophotometer (Jobin Yvon, Grasbrunn, Germany), with excitation and emission wavelengths of mant-nucleotides at 366 and 450 nm, respectively. GDP- and GTP-binding affinities of $MglA^{+}$, $MglA^{G21V}$, and $MglA^{T26/27N}$ were determined by titrating nucleotide-free $MglA^{+}$, $MglA^{G21V}$, or $MglA^{T26/27N}$ to 0.1 μM mGDP or mGTP or mGppNHp (Pharma Waldhof) at 37°C in Buffer M (50 mM Tris pH 7.5, 50 mM NaCl, 1 mM $MgCl_2$, 1 mM DTE, 5% glycerol) monitoring the change in fluorescence. Obtained data points were fitted to a first-order reaction using Grafit5 (Erithacus software) to obtain the dissociation constant, K_d.

Measurement of GTP hydrolysis by [γ-^{32}P]GTP charcoal method

This was performed as described (Brinkmann *et al*, 2002). Briefly, a mix of 1 μM GTP and 60 nM [γ-^{32}P]GTP in Buffer M was supplemented with 4 μM nucleotide-free $MglA^{+}$, $MglA^{G21V}$, or $MglA^{T26/27N}$ to start the intrinsic GTPase reaction at 25°C. For investigation of MglB-stimulated GTP-hydrolysis, catalytic amounts (0.05 μM) or stoichiometric amounts (4 μM) of MglB were added to start the reaction. Aliquots of 10 μl were taken at certain time points and mixed with 400 μl of charcoal solution (50 g l^{-1} charcoal in 20 mM phosphoric acid) to stop the reaction. The charcoal was pelleted and the amount of free $^{32}P_i$ in the supernatant determined by scintillation counting. Data points were fitted to a first-order reaction to obtain k_{obs}.

MglB affinity measurements

Binding affinities of MglB to $MglA^{+}$, $MglA^{G21V}$, and $MglA^{T26/27N}$ loaded with mGDP, mGppNHp, or mGDP/AlF_x (Supplementary data) were determined by polarization measurements at 37°C in Buffer M. For this, 1 μM MglA loaded with the respective nucleotide was titrated with increasing amounts of MglB and the change in polarization signal monitored.

Analytical gel filtration

Complex formation was investigated by analytical gel filtration using a Superdex75 10/300 (GE Healthcare). A total of 1 mg $MglA^{+}$ bound to GDP or GppNHp or GDP/2 mM AlF_x in the presence or absence of 1.5 mg MglB were incubated 15 min at room temperature, applied and eluted with one column volume of Buffer M. The elution profile was recorded and eluted fractions analysed by SDS–PAGE.

Supplementary data

Supplementary data are available at *The EMBO Journal* Online (http://www.embojournal.org).

Acknowledgements

We thank Hans-Ulrich Mösch, Peter Lenz, Eriko Takano and Anke Treuner-Lange for many discussions and practical help. The Max Planck Society, the graduate program 'Intra- and intercellular transport and communication' funded by the German Research Foundation, and the LOEWE Research Center for Synthetic Microbiology supported this work.

Conflict of interest

The authors declare that they have no conflict of interest.

References

Ahmadian MR, Stege P, Scheffzek K, Wittinghofer A (1997) Confirmation of the arginine-finger hypothesis for the GAP-stimulated GTP-hydrolysis reaction of Ras. *Nat Struct Biol* **4:** 686–689

Anderson DC, Gill JS, Cinalli RM, Nance J (2008) Polarization of the *C. elegans* embryo by RhoGAP-mediated exclusion of PAR-6 from cell contacts. *Science* **320:** 1771–1774

Blackhart BD, Zusman DR (1985) 'Frizzy' genes of *Myxococcus xanthus* are involved in control of frequency of reversal of gliding motility. *Proc Natl Acad Sci USA* **82:** 8771–8774

Bos JL, Rehmann H, Wittinghofer A (2007) GEFs and GAPs: critical elements in the control of small G proteins. *Cell* **129:** 865–877

Bourne HR, Sanders DA, McCormick F (1991) The GTPase superfamily: conserved structure and molecular mechanism. *Nature* **349:** 117–127

Bramkamp M, Emmins R, Weston L, Donovan C, Daniel RA, Errington J (2008) A novel component of the division-site selection system of *Bacillus subtilis* and a new mode of action for the division inhibitor MinCD. *Mol Microbiol* **70:** 1556–1569

Brinkmann T, Daumke O, Herbrand U, Kühlmann D, Stege P, Ahmadian MR, Wittinghofer A (2002) Rap-specific GTPase activating protein follows an alternative mechanism. *J Biol Chem* **277:** 12525–12531

Bulyha I, Schmidt C, Lenz P, Jakovljevic V, Hone A, Maier B, Hoppert M, Sogaard-Andersen L (2009) Regulation of the type IV pili molecular machine by dynamic localization of two motor proteins. *Mol Microbiol* **74:** 691–706

Charest PG, Firtel RA (2007) Big roles for small GTPases in the control of directed cell movement. *Biochem J* **401:** 377–390

Cool RH, Schmidt G, Lenzen CU, Prinz H, Vogt D, Wittinghofer A (1999) The Ras mutant D119N is both dominant negative and activated. *Mol Cell Biol* **19:** 6297–6305

Daumke O, Weyand M, Chakrabarti PP, Vetter IR, Wittinghofer A (2004) The GTPase-activating protein Rap1GAP uses a catalytic asparagine. *Nature* **429:** 197–201

Etienne-Manneville S (2004) Cdc42—the centre of polarity. *J Cell Sci* **117:** 1291–1300

Etienne-Manneville S, Hall A (2002) Rho GTPases in cell biology. *Nature* **420:** 629–635

Feig LA (1999) Tools of the trade: use of dominant-inhibitory mutants of Ras-family GTPases. *Nat Cell Biol* **1:** E25–E27

Gasper R, Meyer S, Gotthardt K, Sirajuddin M, Wittinghofer A (2009) It takes two to tango: regulation of G proteins by dimerization. *Nat Rev Mol Cell Biol* **10:** 423–429

Gitai Z, Dye NA, Reisenauer A, Wachi M, Shapiro L (2005) MreB actin-mediated segregation of a specific region of a bacterial chromosome. *Cell* **120:** 329–341

Gremer L, Gilsbach B, Ahmadian MR, Wittinghofer A (2008) Fluoride complexes of oncogenic Ras mutants to study the Ras-RasGap interaction. *Biol Chem* **389:** 1163–1171

Hartzell P, Kaiser D (1991) Upstream gene of the *mgl* operon controls the level of MglA protein in *Myxococcus xanthus*. *J Bacteriol* **173:** 7625–7635

Hodgkin J, Kaiser D (1979) Genetics of gliding motility in *Myxococcus xanthus* (Myxobacterales): two gene systems control movement. *Mol Gen Genet* **171:** 177–191

Huitema E, Pritchard S, Matteson D, Radhakrishnan SK, Viollier PH (2006) Bacterial birth scar proteins mark future flagellum assembly site. *Cell* **124:** 1025–1037

Inclan YF, Vlamakis HC, Zusman DR (2007) FrzZ, a dual CheY-like response regulator, functions as an output for the Frz chemosensory pathway of *Myxococcus xanthus*. *Mol Microbiol* **65:** 90–102

John J, Rensland H, Schlichting I, Vetter I, Borasio GD, Goody RS, Wittinghofer A (1993) Kinetic and structural analysis of the Mg(2+)-binding site of the guanine nucleotide-binding protein p21H-ras. *J Biol Chem* **268:** 923–929

Kaiser D, Crosby C (1983) Cell movements and its coordination in swarms of *Myxococcus xanthus*. *Cell Motil* **3:** 227–245

Koonin EV, Aravind L (2000) Dynein light chains of the Roadblock/LC7 group belong to an ancient protein superfamily implicated in NTPase regulation. *Curr Biol* **10:** R774–R776

Lam H, Schofield WB, Jacobs-Wagner C (2006) A landmark protein essential for establishing and perpetuating the polarity of a bacterial cell. *Cell* **124:** 1011–1023

Leipe DD, Wolf YI, Koonin EV, Aravind L (2002) Classification and evolution of P-loop GTPases and related ATPases. *J Mol Biol* **317:** 41–72

Leonardy S, Bulyha I, Sogaard-Andersen L (2008) Reversing cells and oscillating motility proteins. *Mol Biosyst* **4:** 1009–1014

Leonardy S, Freymark G, Hebener S, Ellehauge E, Sogaard-Andersen L (2007) Coupling of protein localization and cell movements by a dynamically localized response regulator in *Myxococcus xanthus*. *EMBO J* **26:** 4433–4444

Lutkenhaus J (2007) Assembly dynamics of the bacterial MinCDE system and spatial regulation of the Z ring. *Annu Rev Biochem* **76:** 539–562

Mauriello EM, Mouhamar F, Nan B, Ducret A, Dai D, Zusman DR, Mignot T (2010) Bacterial motility complexes require the actin-like protein, MreB and the Ras homologue, MglA. *EMBO J* **20:** 315–326

Mignot T, Merlie Jr JP, Zusman DR (2005) Regulated pole-to-pole oscillations of a bacterial gliding motility protein. *Science* **310:** 855–857

Mignot T, Shaevitz JW, Hartzell PL, Zusman DR (2007) Evidence that focal adhesion complexes power bacterial gliding motility. *Science* **315:** 853–856

Mittal R, Ahmadian MR, Goody RS, Wittinghofer A (1996) Formation of a transition-state analog of the Ras GTPase reaction by Ras-GDP, tetrafluoroaluminate, and GTPase-activating proteins. *Science* **273:** 115–117

Nelson WJ (2003) Adaptation of core mechanisms to generate cell polarity. *Nature* **422:** 766–774

Patrick JE, Kearns DB (2008) MinJ (YvjD) is a topological determinant of cell division in *Bacillus subtilis*. *Mol Microbiol* **70:** 1166–1179

Rafelski SM, Marshall WF (2008) Building the cell: design principles of cellular architecture. *Nat Rev Mol Cell Biol* **9:** 593–602

Scheffzek K, Ahmadian MR, Kabsch W, Wiesmuller L, Lautwein A, Schmitz F, Wittinghofer A (1997) The Ras-RasGAP complex: structural basis for GTPase activation and its loss in oncogenic Ras mutants. *Science* **277:** 333–338

Shapiro L, McAdams HH, Losick R (2009) Why and how bacteria localize proteins. *Science* **326:** 1225–1228

Stephens K, Hartzell P, Kaiser D (1989) Gliding motility in Myxococcus xanthus: *mgl* locus, RNA, and predicted protein products. *J Bacteriol* **171:** 819–830

Sun H, Zusman DR, Shi W (2000) Type IV pilus of *Myxococcus xanthus* is a motility apparatus controlled by the *frz* chemosensory system. *Curr Biol* **10:** 1143–1146

Thanbichler M, Shapiro L (2008) Getting organized—how bacterial cells move proteins and DNA. *Nat Rev Micro* **6:** 28–40

Tong Z, Gao X-D, Howell AS, Bose I, Lew DJ, Bi E (2007) Adjacent positioning of cellular structures enabled by a Cdc42 GTPase-activating protein mediated zone of inhibition. *J Cell Biol* **179:** 1375–1384

Veltel S, Gasper R, Eisenacher E, Wittinghofer A (2008) The retinitis pigmentosa 2 gene product is a GTPase-activating protein for Arf-like 3. *Nat Struct Mol Biol* **15:** 373–380

Vetter IR, Wittinghofer A (2001) The guanine nucleotide-binding switch in three dimensions. *Science* **294:** 1299–1304

Viollier PH, Thanbichler M, McGrath PT, West L, Meewan M, McAdams HH, Shapiro L (2004) Rapid and sequential movement of individual chromosomal loci to specific subcellular locations during bacterial DNA replication. *Proc Natl Acad Sci USA* **101:** 9257–9262

Wittinghofer A, Nassar A (1996) How Ras-related proteins talk to their effectors. *Trends Biochem Sci* **21:** 488–491

Wu SS, Kaiser D (1995) Genetic and functional evidence that type IV pili are required for social gliding motility in *Myxococcus xanthus*. *Mol Microbiol* **18:** 547–558

Yang R, Bartle S, Otto R, Stassinopoulos A, Rogers M, Plamann L, Hartzell P (2004) AglZ is a filament-forming coiled-coil protein required for adventurous motility of *Myxococcus xanthus*. *J Bacteriol* **186:** 6168–6178

Zhang S, Charest PG, Firtel RA (2008) Spatiotemporal regulation of Ras activity provides directional sensing. *Curr Biol* **18:** 1587–1593